Temporal and spatial variability in the aviation NO[subscript x]-related O[subscript 3] impact

Citation: Gilmore, Christopher K, Steven R H Barrett, Jamin Koo, and Qiqi Wang. "Temporal and spatial variability in the aviation NOx-related O3 impact." Environmental Research Letters 8, no. 3 (September 1, 2013): 034027.

As Published: http://dx.doi.org/10.1088/1748-9326/8/3/034027

Publisher: IOP Publishing

Persistent URL: http://hdl.handle.net/1721.1/81430

Version: Final published version: final published article, as it appeared in a journal, conference proceedings, or other formally published context

Temporal and spatial variability in the aviation NO_x-related O_3 impact

2013 Environ. Res. Lett. 8 034027

(http://iopscience.iop.org/1748-9326/8/3/034027)

OPEN ACCESS
IOP PUBLISHING
ENVIRONMENTAL RESEARCH LETTERS
Environ. Res. Lett. **8** (2013) 034027 (8pp)
doi:10.1088/1748-9326/8/3/034027

Temporal and spatial variability in the aviation NO_x-related O_3 impact

Christopher K Gilmore, Steven R H Barrett, Jamin Koo and Qiqi Wang

Laboratory for Aviation and the Environment, Department of Aeronautics and Astronautics, Massachusetts Institute of Technology, Cambridge, MA, USA

E-mail: sbarrett@mit.edu

Received 12 May 2013
Accepted for publication 15 August 2013
Published 4 September 2013
Online at stacks.iop.org/ERL/8/034027

Abstract
Aviation NO_x emissions promote tropospheric ozone formation, which is linked to climate warming and adverse health effects. Modeling studies have quantified the relative impact of aviation NO_x on O_3 in large geographic regions. As these studies have applied forward modeling techniques, it has not been possible to attribute O_3 formation to individual flights. Here we apply the adjoint of the global chemistry–transport model GEOS-Chem to assess the temporal and spatial variability in O_3 production due to aviation NO_x emissions, which is the first application of an adjoint to this problem. We find that total aviation NO_x emitted in October causes 40% more O_3 than in April and that Pacific aviation emissions could cause 4–5 times more tropospheric O_3 per unit NO_x than European or North American emissions. Using this sensitivity approach, the O_3 burden attributable to 83 000 unique scheduled civil flights is computed individually. We find that the ten highest total O_3-producing flights have origins or destinations in New Zealand or Australia. The top ranked O_3-producing flights normalized by fuel burn cause 157 times more normalized O_3 formation than the bottom ranked ones. These results show significant spatial and temporal heterogeneity in environmental impacts of aviation NO_x emissions.

Keywords: aviation, ozone, adjoint

1. Introduction

As the demand for aviation continues to increase, a more complete understanding of the impact of aircraft emissions on the environment is required to make informed aviation policy, design and operational decisions. Aircraft emissions have two primary environmental impacts. First, emissions in the lower as well as upper troposphere increase the concentration of ground-level particulate matter and ozone (Barrett *et al* 2010), which can lead to detrimental human health impacts (Pope 2002, Laden *et al* 2006). Second, aircraft emissions have a range of climate impacts, as has been reviewed by Lee *et al* (2010). This has motivated the development of policy, technology and operational initiatives to reduce the environmental impacts of aviation (FAA 2011, Mahashabde *et al* 2011).

In particular, the atmospheric impact of aviation NO_x emissions has been a focus of previous atmospheric chemistry–transport modeling studies (Lee *et al* 2010). The introduction of additional NO_x, especially at high altitudes, leads directly to the formation of ozone (O_3), one of the naturally occurring greenhouse gases in the atmosphere. The direct ozone radiative forcing (RF) of aviation is approximately equal to (within ~6%) the CO_2 RF of aviation in 2005. We note, however, that the latter RF is due to the whole history of aviation emissions given the long atmospheric lifetime of CO_2, while the direct O_3 RF is only a function of the past ~2 months of emissions (Stevenson and Derwent 2009). Aircraft NO_x emissions also increase the oxidative capacity of the atmosphere due to an increase

in the OH production rate (Kohler 2010). Increasing OH concentrations lead to a decrease in methane lifetime, which subsequently results in a decadal loss in O_3. Lee *et al* (2010) estimates the total RF due to aircraft NO_x emissions at +0.0138 W m^{-2}, where approximately half of the direct (i.e. short-term) ozone RF of +0.0263 W m^{-2} is offset by longer time scale impacts. This letter examines direct O_3 production due to aviation NO_x—which is potentially amenable to operational or routing mitigation measures—but we note that the longer-term effects are also important and there are significant uncertainties in these (Holmes *et al* 2011).

Aircraft NO_x emissions, as compared to other anthropogenic sources, are important because the production efficiency of ozone at cruise altitudes (9–12 km) is higher than the production efficiency at ground level (Stevenson *et al* 2004, Kohler *et al* 2008), and the RF efficiency (forcing per molecule) at cruise altitudes is relatively high (Naik *et al* 2005). Despite the reasonably well understood chemistry of aviation-attributable O_3, decreasing the ozone impact of aviation is complicated by the relatively short ozone lifetimes and the dependency of ozone production and destruction on the local chemical state of the atmosphere and local transport characteristics. Thus, decreasing NO_x emissions in one particular region may not be as effective in reducing aviation's climate impact as decreasing emissions elsewhere, making the optimal mitigation strategy unclear.

Previous (perturbation) studies have focused on the differences in regional impacts of ground-level anthropogenic NO_x emissions, with Naik *et al* (2005) concluding that anthropogenic NO_x reductions in Southeast Asia have the largest impact on total and upper-tropospheric ozone concentrations. Fry *et al* (2012) obtained similar results, but also concluded that reductions in NO_x emissions create atmospheric warming due to the recovery of atmospheric methane given reductions in OH concentrations. Aircraft NO_x focused studies, such as those by Stevenson *et al* (2004) and Kohler *et al* (2008), were bulk region perturbation studies. Stevenson *et al* (2004) examined the size and duration of the O_3 and OH perturbation given aircraft NO_x emissions at different times of year, while Kohler *et al* (2008) perturbed aircraft NO_x emissions within several altitude bins and observed their relative impacts. A more recent perturbation study by Kohler *et al* (2012) showed that forcing attributable to short-term O_3 peaks near the equator when compared to higher latitudes and also determined that the net forcing due to NO_x emissions is positive (i.e. warming).

These perturbation studies were based on taking the difference of forward atmospheric chemistry–transport simulations. Such approaches have the benefit of both being relatively straightforward to implement and show the spatially varying impact of emissions, but only work for perturbations of sufficient size to avoid subtractive errors. A perturbation approach also requires a simulation for every location and time of interest, making the assessment of more than a few locations or times computationally intractable. Here we apply an adjoint sensitivity approach, which results in the sensitivity of an objective function (tropospheric O_3) to NO_x emissions at all locations and times from one simulation. The only previous application of an adjoint sensitivity approach to aviation NO_x–O_3 is given in table 1 of the supporting information of Bowman and Henze (2012), who applied adjoint modeling to determine the contribution of several sectors to the total O_3 instantaneous radiative effect for August 2006; such an approach has not been used in the current context before.

The tropospheric O_3 impact of individual flights has not previously been computed. While operational strategies to mitigate contrails from aviation have previously been investigated, this has not been possible for aviation-attributable O_3 as this requires quantification of impacts at the resolution of a single flight. The aim of this letter is therefore to quantify the O_3 impact of individual civil aviation flights and to quantify the spatial and temporal variability in the impact of aviation NO_x emissions. We also assess the primary chemical production and loss pathways relevant to O_3 and compare aggregate results to previous work. This represents new understanding of the variability in the atmospheric impacts of flights and a step towards estimating the O_3-related benefits of flight-level operational optimization.

2. Methodology

This section describes the modeling techniques applied to determine the spatial and temporal heterogeneity in the aviation-attributable O_3 and the methodology for computing the per flight ozone impacts.

2.1. GEOS-Chem and the GEOS-Chem adjoint

GEOS-Chem was used in this analysis (Bey *et al* 2001). GEOS-Chem is a global chemistry–transport model that includes transport, wet and dry deposition, and gas and aerosol phase chemistry. Gas phase chemistry is solved using the kinetic pre-processor tool (KPP) developed by Damian *et al* (2002). All simulations use a 4° × 5° horizontal grid with 47 vertical layers, which includes pressure levels up to 0.010 hPa. GEOS-Chem is primarily a tropospheric model (i.e. a full chemistry simulation is performed up to the tropopause) where linearized ozone chemistry is used within the stratosphere. Each simulation in this study is for 16 months, where the first four months are used as spin-up.

The GEOS-Chem adjoint model was developed by Henze *et al* (2007). The model was first used for aviation in particular to determine the impact of aircraft emissions on surface air quality by Koo *et al* (2013). Adjoint models, in general, are applied in sensitivity analysis when the (typically single) output quantity of interest is set and the sensitivity of that output to (many) model input parameters is desired. The adjoint approach avoids an ensemble of forward model runs in calculating sensitivities, where only one 'backwards' integrating simulation is required for each output of interest. This is of particular use in studying the impact of aviation given that we are generally interested in total global or regional (e.g. North America, Asia) impacts, where every emissions grid cell is an input. The fundamentals of this approach are described in Errico (1997) for the application of adjoint models in meteorological study.

Anthropogenic emissions inputs for GEOS-Chem are detailed in van Donkelaar *et al* (2008). Aircraft emissions are derived from the methodology presented in Barrett *et al* (2010) and uses the 2005 civil aviation emissions inventory by Simone *et al* (2013). NO_x emissions are given on an NO_2 mass basis where emissions are partitioned by mole fraction. Cruise emissions are partitioned as 90% NO, 9% NO_2, and 1% HONO (Barrett *et al* 2010). Landing/take-off (LTO) emissions are partitioned as 76% NO, 23% NO_2, and 1% HONO (Barrett *et al* 2010). Full-flight emissions (i.e. LTO and cruise emissions) are used in this analysis, where total aircraft NO_x emissions amount to 2.66 Tg(NO_2), annually. We also note that chemistry within aircraft exhaust plumes is neglected, where emissions are assumed to be instantaneously diluted into the local grid cell.

2.2. Sensitivities to aircraft emissions

The quantity of interest is the annually averaged O_3 perturbation due to aircraft NO_x emissions, which is given by

$$\delta O_3 = \frac{1}{T}\sum_{i=1}^{N_{\mathrm{LAT}}}\sum_{j=1}^{N_{\mathrm{LON}}}\sum_{k=1}^{N_{\mathrm{TROP}}}\sum_{t=1}^{T}\left[\frac{\partial J}{\partial E_{\mathrm{NO}_x}(i,j,k,t)} \times E_{\mathrm{NO}_x}(i,j,k,t)\right], \quad (2.1)$$

where E_{NO_x} is the time-varying three-dimensional emissions matrix, T is the number of time steps within the (one year) period over which O_3 impacts are averaged, N_{LAT} is the number of latitude grid cells, N_{LON} is the number of longitude grid cells, N_{TROP} is the number of troposphere altitude layers, and $\partial J/\partial E_{\mathrm{NO}_x}$ is the adjoint sensitivity with objective function

$$J = \sum_{i=1}^{N_{\mathrm{LAT}}}\sum_{j=1}^{N_{\mathrm{LON}}}\sum_{k=1}^{N_{\mathrm{TROP}}}\sum_{t=1}^{T} M_{\mathrm{O}_3}(i,j,k,t), \quad (2.2)$$

with M_{O_3} being the mass of O_3 in a model grid cell. The adjoint sensitivity $\partial J/\partial E_{\mathrm{NO}_x}$— a four-dimensional matrix— is therefore the total subsequent change in tropospheric O_3 burden given 1 kg of NO_x emitted at a location i, j, k and time t.

Applying first-order sensitivities in estimating impacts assumes a linear relationship between the specie of interest and aircraft emissions at the level of the perturbation being considered. This assumption has been shown to be valid for the O_3 response to total aircraft NO_x for a range of emissions perturbations in magnitude and altitude (Kohler *et al* 2008). We infer that the linear approximation is at least as valid for individual flights as for all aviation NO_x. Diurnal variations in sensitivities are not considered in this analysis as the daily variations in ozone production from aircraft NO_x emissions was <2% of the seasonal variation based on a spectral (FFT) analysis of aircraft NO_x emissions-weighted sensitivity data. This is not necessarily true of ground-level sensitivities.

2.3. Chemical pathways analysis

In order to determine the primary drivers behind the temporal as well as spatial patterns of the calculated ozone sensitivities, a simplified analysis of the underlying chemistry in the forward simulations is performed. The time rate of change for any given specie within a chemical kinetic system is the difference between the total production and loss rates. Each production and loss rate in turn is a function of the product of the rate coefficient and the relevant species concentrations (Seinfeld and Pandis 2006). Solving chemical kinetics represents a challenge given the stiffness of the system (i.e. orders of magnitude differences in reaction rate time scales), where implicit methods are used to avoid small time steps (Hairer and Wanner 2002). Here, a simplified approach is taken to quantify each pathway's contribution. The total ozone rate of change is disaggregated into its most significant production and loss pathways (significant being ~5% of the total rate within the chemistry time step). A weighted average is then performed for each pathway during chemistry in order to determine a characteristic rate of change for that one hour time step, where the weightings are determined by the length of the sub-time steps (which sum to one hour) required to maintain convergence of the solver. These weighted averages are then directly compared for different locations and times to approximately quantify how the time evolution of the aviation-attributable O_3 is determined by the underlying chemistry. The pathways considered in this analysis are stated in table 1. Note that reaction (1) in GEOS-Chem is combined with NO_2 photolysis to form a single chemical reaction ($NO_2 \rightarrow NO + O_3$), which implicitly includes atomic oxygen's reaction with molecular oxygen to produce O_3. In addition, reactions (1) and (2) are combined to form the 'production' pathway as they are primary source and sink, respectively, of O_3 in the troposphere and their net rate determines the ozone production rate within the troposphere. This pathway is further discussed in section 3.1.

Table 1. Pathways of O_3 production and loss considered in the chemical pathway analysis.

Pathway
(1) $O + O_2 + M \rightarrow O_3 + M$
(2) $O_3 + NO \rightarrow NO_2 + O_2$
(3) $O_3 + OH \rightarrow HO_2 + O_2$
(4) $O_3 + HO_2 \rightarrow OH + 2O_2$
(5) $O_3 + NO_2 \rightarrow NO_3 + O_2$
(6) $O_3 + h\nu \rightarrow O_2 + O(^1D)$
(7) Dry deposition

2.4. Calculating the impact of individual flights

Once four-dimensional sensitivity data have been calculated, the first-order atmospheric response of O_3 concentrations to aircraft NO_x emissions can be estimated. The aircraft emissions model by Simone *et al* (2013) generates three-dimensional emissions matrices for each aircraft type flown between a pair of airports. Following the generation of the gridded emissions data for a particular scenario, the first-order response can then be determined by taking the inner product (i.e. component-wise multiplication and summation) between

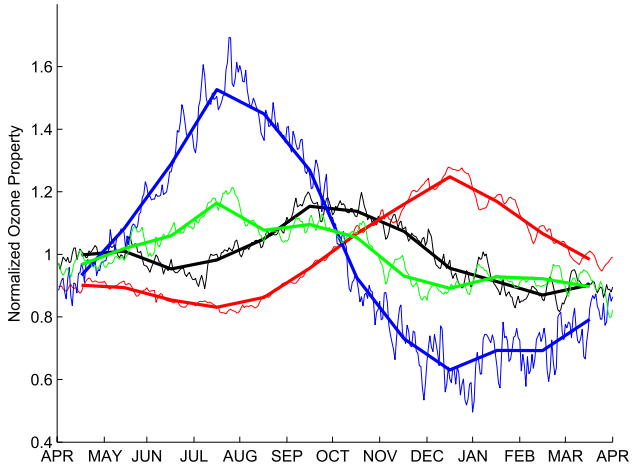

Figure 1. Sensitivity of total tropospheric O_3 to aviation NO_x emissions (black); ozone production efficiency (blue) weighted by aviation NO_x emissions; aviation-attributable ozone production rate (green); aviation-attributable ozone lifetime (red); all with one month averages (thick line) and normalized by annual mean, which is 3.2 kg O_3 / kg NO_x (black), 17.5 (blue), 1375 molecules cm^{-3} s^{-1} (green), 26.9 days (red).

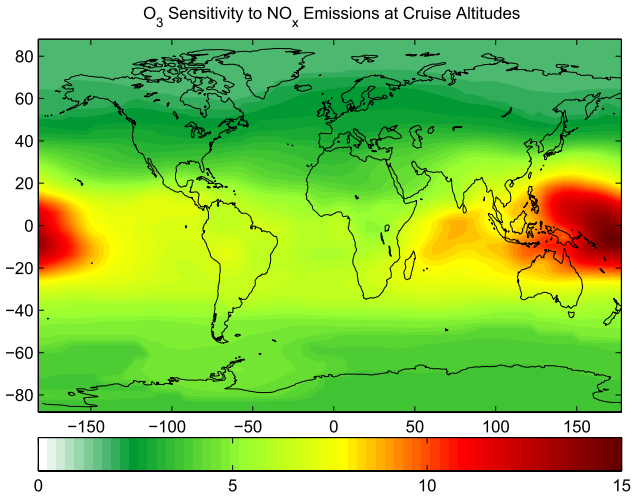

Figure 2. Annual average sensitivity of total tropospheric O_3 to cruise NO_x emissions (9–12 km) in kg(O_3) / kg(NO_x).

the sensitivity (for a particular day of the year) and emissions matrices, as indicated in equation (2.1). This process, which is computationally inexpensive compared to a complete forward model simulation, allows for the rapid calculation of the atmospheric impacts associated with each flight.

3. Results

This section presents the results from the adjoint sensitivity simulations using the cost function definition in equation (2.2) and the chemical pathway analysis. A forward model analysis was performed with and without aircraft emissions to compare GEOS-Chem with previous aviation NO_x studies. GEOS-Chem predicts an annually averaged O_3 perturbation of 0.8 DU as compared to 0.9 DU estimated by Kohler *et al* (2008). Using the GEOS-Chem adjoint-calculated ozone sensitivities multiplied by total aviation NO_x emissions results in an annually averaged O_3 perturbation that is 10% lower than the forward model result, consistent with the weak nonlinearity found in previous studies.

3.1. Sensitivity of ozone burden to aircraft emissions

From the GEOS-Chem adjoint model, the sensitivity of total tropospheric O_3 to NO_x emissions is calculated. Figure 1 shows the average effect of 1 kg of aircraft NO_x emitted as a function of time of year on the annual average tropospheric O_3 burden in kg (black). This was computed by taking the aviation NO_x emissions-weighted average of the sensitivity matrix for each hour of the year (then averaging over one year). The results show that aviation NO_x emissions in October cause 40% more annually averaged tropospheric O_3 than emissions in April. Stevenson *et al* (2004) also showed a peak ozone perturbation given an aircraft NO_x perturbation in October.

Figure 2 shows the sensitivity of annually averaged tropospheric O_3 to NO_x emissions at cruise altitudes (9–12 km average), where the sensitivity has been averaged over a year. The peak sensitivity is over the Pacific at 4°S, 170°E (∼1000 km northeast of the Solomon Islands). In this location an emission of 1 kg of aircraft NO_x would result in a 15 kg increase in O_3 burden averaged over one year. This is 5.1 times higher than the sensitivity in Europe and 3.7 times higher than North America. This peak in sensitivity in the equatorial region is consistent with recent forward modeling results by Kohler *et al* (2012). It is also consistent with the results presented in Stevenson and Derwent (2009) which showed peak short-term O_3 integrated RF impacts in the remote Pacific region. High sensitivities were associated with NO_x-scarce regions (e.g. remote Pacific), as was the case in this analysis. We note from figure 2 that the 'center of mass' of the sensitivity is south of the equator, indicative of the weighting between both NO_x scarcity and solar zenith angle in ozone sensitivity.

The chemical pathway analysis is used to investigate these temporal and spatial variations. The rate of change of aviation-attributable ozone is approximated as

$$\frac{\mathrm{d}(\delta \mathrm{O}_3)}{\mathrm{d}t} \approx \left.\frac{\mathrm{d}(\mathrm{O}_3)}{\mathrm{d}t}\right|_{\mathrm{av}} - \left.\frac{\mathrm{d}(\mathrm{O}_3)}{\mathrm{d}t}\right|_{\mathrm{w/o\ av}}, \qquad (3.1)$$

where av denotes the rate of change of O_3 with aviation, w/o av denotes the rate of change without aviation, and δO_3 denotes the O_3 perturbation attributable to aircraft emissions.

The pathways in figure 3 account for 86% of total net rate of change of aviation-attributable O_3, while all the pathways considered in the analysis overestimate net production by 3%. The 'Production' pathway is the net O_3 production resulting from the direct generation of O_3 by $O + O_2$ (where atomic oxygen is generated by way of NO_2 photolysis) minus the destruction due to ozone's reaction with NO (which tracks well with the rate of the $HO_2 + NO$ reaction).

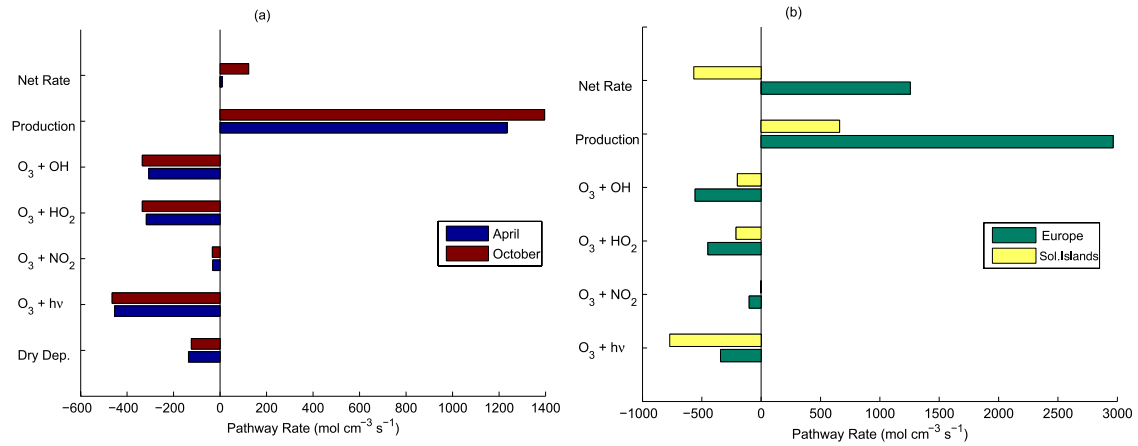

Figure 3. Change in aviation-only O_3 production and loss pathways for (a) aviation emissions in October relative to April and (b) cruise altitude NO_x emissions near the Solomon Islands relative to Europe.

Figure 3(a) shows the primary pathways that drive the temporal pattern in the averaged sensitivity when comparing pathway rates in October (peak sensitivity) to April (minimum sensitivity). We note that 'April' in figure 3 is an average across the first and last month's sensitivities given that they are not exactly cyclical (figure 1). It can be seen that while overall production rates in October are higher, chemical and photolytic loss rates are also larger in magnitude, thus the higher production rate is offset ∼30% by the higher loss rates, which is chemically dominated by ozone's reaction with OH. Figure 3(a) shows that while lifetimes in April may be longer (i.e. loss rates are lower), this does not correspond to peak ozone sensitivity to aircraft NO_x emissions. The low loss rates in the winter months, however, do correspond with the peak in the aviation-attributable O_3 perturbation.

Figure 3(b) shows the relative change in each pathway for the location of peak sensitivity in the Pacific near the Solomon Islands relative to the average for Europe. The spatial difference is driven by decreased total production (photolysis) as well as increased $O_3 + HO_2$ loss, decreased $O_3 + OH$ loss, and increased photolytic loss. This follows from the NO_x-scarce environment in the remote Pacific. Loss due to HO_2 is more prevalent in this region given that NO_x is not present to cycle HO_2 to OH, resulting in a lower O_3+OH loss rate. Given that the overall production rate is also lower (i.e. $HO_2 + NO$ is not as significant), this suggests that O_3 production is NO limited, thus resulting in higher ozone sensitivities in this region. Note that the positive $O_3 + HO_2$ loss rate indicates a decrease in ozone loss by way of HO_2 when aviation emissions are introduced. In addition, pathway rates are higher in the case of figure 3(b) as only chemistry at cruise altitudes is being considered, where rates are in general higher for aviation-attributable ozone at this altitude range as opposed to production or loss rates in the lower troposphere.

As fully spatially resolved sensitivity data is generated (having been averaged in time), ground-level sensitivities are also compared to previous studies that investigated the impact of changing ground-level anthropogenic NO_x emissions. Our results generally agree with the previous studies, indicating that sensitivities are highest in Southeast Asia while the overall temporal patterns show consistently high sensitivities in the boreal summer and early autumn months and minimum sensitivities in the winter. Naik *et al* (2005) estimated a factor of 9 difference between the magnitude of sensitivities for Southeast Asia relative to North America for global O_3 due to changes in regional NO_x emissions, whereas a factor of ∼2 is found here when calculating spatially averaged sensitivities. The magnitudes of the sensitivity values, however, approximately correspond to the sensitivity values calculated by Fry *et al* (2012) where ozone sensitivities are on the order of 1 kg O_3 /kg NO_x.

3.2. Comparison to ozone production efficiency

The sensitivity results presented in figure 2 also provide an alternative measure to the more common ozone production efficiency (OPE). The concept of OPE was introduced by Liu *et al* (1987). In this analysis, however, we use the definition presented in Seinfeld and Pandis (2006) and define OPE (in a simplified atmosphere) as

$$\mathrm{OPE} = \frac{k_{\mathrm{HO_2+NO}}[\mathrm{HO_2}][\mathrm{NO}]}{k_{\mathrm{NO_2+OH}}[\mathrm{NO_2}][\mathrm{OH}]}. \tag{3.2}$$

Equation (3.2) thus defines OPE to be the ratio of the time rate of O_3 production (approximated by the rate of the additional production of NO_2) to the time rate of NO_x removal (i.e. HNO_3 production). This definition does not capture the impact of O_3 removal pathways, but rather is a reflection of the likelihood of NO_x to promote O_3 production rather than exit the ozone cycle through nitric acid production. In addition, OPE is an instantaneous measure of the production tendency of NO_x, where longer-term atmospheric impacts are not captured. The adjoint sensitivity, however, represents the total expected net production of O_3 and its lifetime induced by a small increment in NO_x concentration at a particular time and location in the atmosphere. Figure 1 shows OPE plotted (in blue) versus the previously calculated ozone sensitivity.

The respective peaks of OPE and O_3 sensitivity do not coincide. OPE peaks in the (boreal) summer months where photolysis of NO_2 is most active, preceding the sensitivity

Table 2. Ranking of top five flights by O_3 impact for two different metrics. The first section shows ranking by total impact, i.e. the contribution of each flight to the total ozone perturbation. The second section shows ranking by FOF, i.e. ozone impact normalized by fuel burn and scaled by the lowest impact flight. Return trips were not counted (only the higher of a return-trip pair are counted).

Rank	Origin	Destination	Aircraft	Total O_3 (kg)	FOF
		Ranked by total impact			
1	Sydney, Australia	Bombay, India	B747	25 300	111
2	Honolulu, HI, USA	Sydney, Australia	B747	24 300	130
3	Auckland, New Zealand	Seoul, South Korea	B777	22 900	157
4	Sydney, Australia	Tokyo, Japan	B747	22 400	129
5	Auckland, New Zealand	Los Angeles, CA, USA	B747	22 100	101
		Ranked by FOF			
1	Auckland, New Zealand	Seoul, South Korea	B777	22 900	157
2	Sydney, Australia	Seoul, South Korea	B777	18 200	146
3	Sydney, Australia	Bangkok, Thailand	B777	17 600	144
4	Brisbane, Australia	Bangkok, Thailand	B777	14 900	139
5	Christchurch, New Zealand	Seoul, South Korea	B777	19 700	139

peak by 2–3 months. When comparing OPE and the ozone sensitivities to the chemical pathway analysis, we see that the OPE tracks closely with the total O_3 production rate. The lower loss rate (and longer lifetime) in the winter means that the peak ozone sensitivity to aircraft NO_x emissions is between the two—in October where there is a balance between declining ozone production and increasing lifetime as illustrated in figure 3(a). This is further demonstrated in figure 1, where a curve corresponding to O_3 lifetime is also shown (calculated by instantaneous burden divided by instantaneous loss rate).

4. Aviation's O_3 impact by flight

This section presents the results from the application of per flight emissions data to the generated O_3 sensitivities. The highest impact flights in terms of ozone are found as well as their marginal impact to the cumulative O_3 perturbation.

The impact of aviation NO_x emissions on a per flight basis is calculated through the use of adjoint sensitivities for the total atmospheric ozone burden previously calculated. Results are normalized on three different bases: no normalization, by seat-km, and by fuel burn. The third normalization is also scaled such that the minimum value across all flights is one. We call this quantity the 'flight ozone factor' (FOF) and are taken relative to the annually averaged minimum. For this analysis, only aircraft with capacities greater than 70 passengers are considered as the reliability of the fuel burn data for some of the smaller aircraft is unknown. In addition, flights under 200 km are excluded to limit the number of short range movements of large aircraft. This equates to approximately 83 000 unique flights.

Table 2 shows the five highest flights by total atmospheric ozone impact and FOF. For total O_3 generated by a flight, it follows that the highest impact flights occur in the geographical area with the largest ozone sensitivities throughout the flight, which are concentrated in Southeast Asia and Australia. These flights also correspond to large aircraft (predominately 777s and 747s), relatively long flights, and thus NO_x production will be relatively large due to the amount of fuel burnt. In addition, all flights, whether ranked by total impact or FOF, have origins or destinations in Australia or New Zealand. Within the top five, however, only one flight appears for both normalizations (Auckland to Seoul). The highest O_3 impact flight on a fuel burn-normalized basis results in approximately 157 times more O_3 than the lowest impact flight. However, because fuel burn also varies by two orders of magnitude across flights, the highest impact flights result in four orders of magnitude greater O_3 production than the lowest impact flights.

Table 3. Total ozone impact normalized by seat-km.

Rank	Origin	Dest.	Aircraft	kg/st-km
1	Mauritius	Saint Denis	B777	0.018
2	Montevideo	Buenos Aires	B747	0.013
3	Mauritius	Saint Denis	A340	0.013
4	Arequipa	Juliaca	B727	0.012
5	Rio De Janeiro	Sau Paulo	B777	0.011

Table 2 also shows that the flights with the highest total impact do not necessarily correlate to the flights with the highest impact on a fuel burn basis. Dividing by fuel burn roughly normalizes the flight by distance for a comparably sized aircraft. Thus, flights that remain within the Australia–Southeast Asia area result in large FOFs, while a flight such as Auckland to Los Angeles generates a lower FOF since a portion of the flight is spent outside this high sensitivity zone.

Table 3 shows the annually averaged O_3 impact for the top five flights normalized by seat-km. Results are dominated by large aircraft flying short distances such as from Mauritius to Saint Denis. Spatially, the majority of these flights occur in South America or Southeast Asia, although many of the flights from Mauritius to Saint Denis (islands near Madagascar) rank highly using this normalization.

We find that the top (500, 5000, 50 000) unique flights ranked by O_3 impact create (11.3, 47.7, 93.7)% of the total O_3 impact while constituting (5, 36, 91)% of the seat-km and

(0.6, 6, 60)% of the unique flights. Thus the first (500, 5000, 50 000) unique flights are (18.8, 7.8, 1.6) times as effective per seat-km at creating O_3 than the average flight per seat-km.

5. Discussion

Previously, perturbation studies have been used to investigate the impact of aviation emissions in different locations and times, particularly with respect to the impact of NO_x emissions on tropospheric ozone burdens. These studies have been largely restricted to bulk regions or particular injection times due to limitations inherent in forward sensitivity analyses in this context. In this study, an adjoint approach is used to determine the full four-dimensional sensitivity of tropospheric ozone to NO_x emissions using the GEOS-Chem adjoint model. Using this approach per flight impacts were determined.

While ozone production related to aviation peaks in the boreal summer, aviation NO_x emissions in the autumn are most effective at increasing the annual averaged tropospheric O_3 burden. This occurs at approximately the midpoint between the peak in ozone production and the peak in ozone lifetime associated with aviation NO_x emissions. On a spatial basis, cruise altitude NO_x emissions near the Solomon Islands would contribute 5.1 times more to the annual averaged tropospheric O_3 burden than emissions over Europe. More importantly, sensitivities in Southeast Asia—where aviation is growing significantly faster than the global average—are more than double those in North America and Europe. This implies that the marginal impact of aviation growth in future will be greater than the historical growth that has been concentrated in North America and Europe.

Our analysis showed that the highest total ozone perturbations were caused by individual flights with origins and destinations in Australia or New Zealand, which was also true if results were normalized by total fuel burn. Using this metric, the most impactful flight (of the 83 000 unique flights considered) creates 157 times more ozone per kg of fuel burned than the minimum. These flights also correspond to areas of high ozone sensitivity to NO_x emissions and flight paths largely contained within high sensitivity regions. We also find that a disproportionate fraction of the direct ozone impact from aviation can be attributed to a relatively small fraction of flights. The strength of the spatial and temporal variability in ozone production due to aviation NO_x emissions raises the possibility of time and location dependent mitigation measures, which may be facilitated by the four-dimensional sensitivity data created in this analysis. We note other atmospheric impacts associated with aircraft emissions also need to be considered and will be the subject of future work. As Stevenson and Derwent (2009) showed, the longer-term CH_4 climate response may outweigh the near-term O_3 perturbation due to aircraft emissions.

Acknowledgments

The US Federal aviation administration funded part of this work. We thank Christopher J Sequeira for his management of the project. Any findings are those of the authors and may not represent the views of the FAA. CKG was also supported by the John and Irene M Goldsmith scholarship at the MIT Department of Aeronautics and Astronautics.

References

Barrett S R H, Britter R and Waitz I A 2010 Global mortality attributable to aircraft cruise emissions *Environ. Sci. Technol.* **44** 7736–42

Bey I, Jacob D J, Yantosca R M, Logan J A, Field B D, Fiore A M, Li Q, Liu H Y, Mickley L J and Schultz M G 2001 Global modeling of tropospheric chemistry with assimilated meteorology: model description and evaluation *J. Geophys. Res.* **106** 23073–95

Bowman K and Henze D K 2012 Attribution of direct ozone radiative forcing to spatially resolved emissions *Geophys. Res. Lett.* **39** L22704

Damian V, Sandu A, Damian M, Potra F and Carmichael G 2002 The kinetic preprocessor KPP-a software environment for solving chemical kinetics *Comput. Chem. Eng.* **26** 1567–79

Errico R M 1997 What is an adjoint model? *Bull. Am. Meteorol. Soc.* **78** 2577–91

Federal Aviation Administration 2011 *Destination 2025* (www.faa.gov/about/plans_reports/media/Destination2025.pdf)

Fry M M *et al* 2012 The influence of ozone precursor emissions from four world regions on tropospheric composition and radiative climate forcing *J. Geophys. Res.* **117** D07306

Hairer E and Wanner G 2002 *Solving Ordinary Differential Equations II: Stiff and Differential-Algebraic Problems* (Berlin: Springer)

Henze D K, Hakami A and Seinfeld J H 2007 Development of the adjoint of GEOS-Chem *Atmos. Chem. Phys.* **7** 2413–33

Holmes C D, Tang Q and Prather M J 2011 Uncertainties in climate assessment for the case of aviation NO *Proc. Natl Acad. Sci. USA* **108** 10997–1002

Kohler M O 2010 Chemistry of the atmosphere and impacts from global aviation *Encyclopedia of Aerospace Engineering* ed R Blockley and W Shyy (New York: Wiley)

Kohler M O, Radel G, Dessens O, Shine K P, Rogers H L, Wild O and Pyle J A 2008 Impact of perturbations to nitrogen oxide emissions from global aviation *J. Geophys. Res.* **113** D11305

Kohler M O, Radel G, Shine K P, Rogers H L and Pyle J A 2012 Latitudinal variation of the effect of aviation NO_x emissions on atmospheric ozone and methane and related climate metrics *Atmos. Environ.* **64** 1–9

Koo J, Wang Q, Henze D K, Waitz I A and Barrett S R H 2013 Spatial sensitivities of human health risk to intercontinental and high-altitude pollution *Atmos. Environ.* **71** 140–7

Laden F, Schwartz J, Speizer F E and Dockery D W 2006 Reduction in fine particulate air pollution and mortality: extended follow-up of the harvard six cities study *Am. J. Respir. Crit. Care. Med.* **173** 667–72

Lee D S *et al* 2010 Transport impacts on atmosphere and climate: aviation *Atmos. Environ.* **44** 4678–734

Liu S C, Trainer M, Fehsenfeld F C, Parrish D D, Williams E J, Fahey D W, Hubler G and Murphy P C 1987 Ozone production in the rural troposphere and the implications for regional and global ozone distributions *J. Geophys. Res.* **92** 4191–207

Mahashabde A *et al* 2011 Assessing the environmental impacts of aircraft noise and emissions *Prog. Aerosp. Sci.* **47** 15–52

Naik V, Mauzerall D, Horowitz L, Schwarzkopf M D, Ramaswamy V and Oppenheimer M 2005 Net radiative

forcing due to changes in regional emissions of tropospheric ozone precursors *J. Geophys. Res.* **110** D24306

Pope C A 2002 Lung cancer, cardiopulmonary mortality, and long-term exposure to fine particulate air pollution *J. Am. Med. Assoc.* **287** 1132–41

Seinfeld JH and Pandis S N 2006 *Atmospheric Chemistry and Physics* (Hoboken, NJ: Wiley)

Simone N W, Stettler M E J and Barrett S R H 2013 Development of a rapid global aircraft emissions estimation tool with uncertainty quantification *Trans. Res.* D **25** 33–41

Stevenson D S and Derwent R G 2009 Does the location of aircraft nitrogen oxide emissions affect their climate impact? *Geophys. Res. Lett.* **36** L7810

Stevenson D S, Doherty R M, Sanderson M G, Collins W J, Johnson C E and Derwent R G 2004 Radiative forcing from aircraft NO_x emissions: mechanisms and seasonal dependence *J. Geophys. Res.* **109** D17307

van Donkelaar A *et al* 2008 Analysis of aircraft and satellite measurements from the intercontinental chemical transport experiment (INTEX-B) to quantify long-range transport of East Asian sulfur to Canada *Atmos. Chem. Phys.* **8** 2999–3014